Journal of Imaging Science and Technology® 56(5): 050502-1–050502-14, 2012.
© Society for Imaging Science and Technology 2012

A Relative Perceived Visual Contrast Model for High Dynamic Range Photography

M. James Shyu▲
Department of Information Communications, Chinese Culture University, Taipei, Taiwan
E-mail: mjshyu@faculty.pccu.edu.tw

Yoichi Miyake▲
Research Center for Frontier Medical Engineering, Chiba University, Chiba, Japan

Abstract. *A relative perceived visual contrast (RPVC) model is proposed for high dynamic range (HDR) photography. This approach assumes that an equivalence of perceived visual contrast can be implemented between HDR and low dynamic range (LDR) images. An RPVC function is derived in this study to perform the visual contrast mapping, which provides uncomplicated but effective transformation to compensate for the luminance change in the HDR environment. Other essential features such as the bilateral-type filter and computation in IPT color spacing found in prior HDR models are also incorporated. A specially designed lighting environment was configured to generate a real HDR scene not only for the purpose of model developing but also for psychophysical evaluation. Six other HDR models were compared by the paired comparison method in a real scene. Further comparisons were performed between iCAM06 and this RPVC model for computation efficiency. The results indicate that this RPVC model is effective and that it may bring a new thought to HDR research.* ©2012 Society for Imaging Science and Technology.
[DOI: 10.2352/J.ImagingSci.Technol.12.56.5.050502]

INTRODUCTION

It is well known to the experienced photographer that, when the dynamic range of a scene is higher than the limited dynamic range of the recording photographic medium, the resulting photo will be missing the details of either high light or shadow. It is crucial for the photographer to take this restriction into consideration. To go beyond this limitation, Ansel Adams applied his famous "Zone System" concept along with superb darkroom techniques to control the tone-reproduction characteristics, and he made fabulous black-and-white photos under many extreme lighting conditions, like scenes ranging from bright snow under direct sunlight to dark objects in deep shadow.[1–3] Nowadays photos taken in such extreme conditions are referred to as high dynamic range (HDR) images.

Ansel Adams reproduced his images subjectively in a "pre-visualization"[4] way that is guided by his personal view which can be considered as a preferred, more pleasing, reproduction. However, for objective reproduction, a specific quantitative process is more desirable for HDR situations. In the computer graphics community, there was an early HDR publication at SIGGRAPH in 1984 by Miller and colleagues about keeping brightness ratios constant as a global tone-reproduction model.[5] Consequent HDR works are referred to as tone-mapping operators (TMOs) which incorporate computing algorithms for processing computer graphic data. From the imaging science's standpoint, Land and McCann proposed the Retinex theory in 1967 with the concept of center/surround (or center/background in more recent convention) spatially opponent operation on color patches.[6] Several newly improved Retinex-based HDR image-reproduction models have been published lately specifically for pixel-based images.[7–10]

In the meantime, based on experimental data from solid color patches, CIE recommended both CIELAB and CIELUV uniform color spaces in 1976. Much research effort has been coordinated on the color appearance model, resulting in the recommendations of the CIECAM97 and the consequent CIECAM02 color appearance models. However, it was known that these models were derived by solid color patch-type stimulus, not pictorial color images. On the other hand, S-CIELAB was proposed to incorporate spatial filtering for considering the spatial property in image color differences.[11] Furthermore, Fairchild proposed a new image color appearance model (iCAM) handling the spatial property and many other attributes of the stimuli in the pictorial image.[12,13] A consequently enhanced model, iCAM06, was then proposed and applied in HDR image reproduction with color appearance features from the CIE color appearance models.[14,15]

Essentially, TMOs rely on the mapping of specific attributes to compress the dynamic range globally or locally. For example, Tumblin and Rushmeier's[16] brightness-based operator seeks to match the suprathreshold brightness appearance across the range of scene luminance. This operator attempts to achieve the mapping between HDR and LDR by preserving the brightness values. More examples of the TMOs are listed in Table I. Meanwhile, Retinex-type algorithms process the image with the center/surround characteristics of the human visual system. Image appearance models like iCAM06, provide very complete and complicated methods to cope with the issues of visual appearance. Each of the HDR models has its own merit and flavor in processing the image. A very complete and detailed description of all

▲ IS&T Members.

Received Jul. 11, 2011; accepted for publication Nov. 17, 2012; published online Jan. 21, 2013.
1062-3701/12/56(5)/050502/14/$20.00

Table I. Sampling of prior HDR image-processing models.

Year	Authors	Characteristics
1984	Miller[5]	Mapping by constant brightness ratio
1993	Tumblin–Rushmeier[16]	Mapping brightness value at suprathreshold level
1993	Chiu[19]	First spatially varying operator
1994	Ward[20]	Matches contrast sensitivity over photopic threshold
1996	Ferwerda[21]	Matches contrast sensitivity at scotopic visibility
1997	Ward-Larson[22]	Histogram mapping
1998	Pattanaik[23]	Multi-scale for threshold and suprathreshold vision
2002	Reinhard[24]	Photographic tone mapping
2002	Ashikhmin[25]	Mapping by local contrast equivalence
2002	Durand–Dorsey[26]	Fast bilateral filter
2002	Fattal[27]	Attenuating large gradient for compression
2002	Kotera[7]	Adaptive scale-gain MSR Retinex
2002	Fairchild[12]	iCAM image appearance
2004	Rahman[8]	Multi-scale Retinex with color restoration (MSRCR)
2005	Reinhard–Devlin[28]	Photoreceptor model
2007	Meylan[9]	Retinal local adaptation of color filter array images
2007	Wang[10]	Integrated surround Retinex
2007	Kuang[14]	iCAM06 image appearance
2009	Lu[29]	Full range contrast perception model
2009	Shyu[30]	Perceived visual contrast mapping locally

recent HDR models can be found in Reinhard's books.[17,18] Sampling of these prior HDR image-processing models and their main characteristics are listed in Table I.

Many prior publications evaluating the performance of HDR image-reproduction models gave very good insight regarding what HDR processing should be considered and how the verifications could be performed.[31–37] It is known that the bilateral filter is a key feature to avoid the "halo" problem.[26] In addition, both Ledda[32] and Yoshida[35] indicated that, when conducting psychophysical experiments to compare these models, observers behaved differently with and without a referencing image. Furthermore, when a real scene is present as a reference, the fast bilateral filtering method seems to generate higher contrast and more visibility of detail than in the reference image.[32,35] It is reported that iCAM reproduced the images with less local contrast and less colorfully compared with the original scenes.[15] They all reveal an important indication that the control of the contrast attribute deserves further study when matching an HDR image with a real scene.

Meanwhile iCAM06 consistently showed a better performance than the other models with enhancements from the previous iCAM. These enhancements include a bilateral filter, photoreceptor response function and a luminance-dependent local contrast function.[15] It is also well known to the experienced photographer that a proper handling of contrast is an important clue to revealing the lighting conditions of the scene. Hunt also stated that "images never look right unless their contrasts are correct".[38] Learning from all the prior wisdom, this newly proposed model is based on the iCAM framework with enhancement of perceived visual contrast mapping. The derivation of the perceived visual contrast mapping concept is specified in more detail here compared with the previous publication of the same authors.[30] Statistical analysis of the paired comparison has been performed more precisely in this article. Several LDR images were captured in common photography practice, such as sunrise, sunset, back-lighting, indoor/outdoor as well as panoramic views, and then processed both by this proposed model and iCAM06 to be viewed side by side for direct visual reference to provide a cross-check for the readers.

Contrast Attribute

Contrast is a unique attribute that has been referred to in various ways.[39–44] In tone reproduction, where original and reproduced images are both present, image contrast is defined as follows.

The rate of change of the relative luminance of image elements of a reproduction as a function of the relative luminance of the same image elements of the original image.[41,42]

In visual science, contrast is defined as follows.

The difference between minimum and maximum luminance in an image.[41,42]

The second definition is more applicable to HDR images, where a direct description of image contrast from the image itself is desirable. Another general form to define a two-dimensional pattern for contrast measure mathematically, known as the Michelson[39] contrast, is

$$C_m = (L_{\max} - L_{\min})/(L_{\max} + L_{\min}), \qquad (1)$$

where $L_{\max}$ and $L_{\min}$ are the maximum and the minimum luminance values; this is commonly referred to as physical contrast. However, Michelson's definition is considered as a global contrast measure since only the global parameters like the maximum and the minimum values are needed. Moreover, Calabria and Fairchild[45,46] indicated that the preferred perceived image contrast is a function of multiple image characteristics as opposed to simply being a function of the dynamic range of intensity (or maximum and minimum luminance). This indicates the existence of a certain relation between the physical image attribute (luminance) and the perceived contrast.

In addition the Stevens effect states that perceived contrast increases with increasing luminance level.[44,47] This is especially important since in the HDR environment the scene luminance can be from 0.001 cd/m^2 under faint starlight to 100 cd/m^2 for indoors or to 100,000 cd/m^2 for bright sunlight.[48] The luminance range of the reproduction media can be on different levels as well.

Wandell[49] also pointed out that the image contrast, not the absolute light level, is the most important information represented by the visual pathways, and the image contrast is defined as the ratio of the local intensity and the average image intensity. This is very similar to the Retinex theory

Table II. Estimated data points (normalized to between 0 and 1) sampled from perceived contrast curves in Burkhardt[50] at five levels of background luminance.

Background luminance (cd/m^2)	0.017	0.17	1.55	17	200
Luminance (physical) contrast	Normalized perceived visual contrast				
0	0	0	0	0	0
0.2	0.28	0.28	0.28	0.28	0.28
0.3	0.37	0.37	0.37	0.37	0.37
0.6	0.47	0.49	0.53	0.59	0.65
0.8	0.52	0.55	0.64	0.74	0.85
1	0.55	0.62	0.74	0.86	1

in taking the ratio of the signal at any given point and normalizing it with a weighted average of the signals in that retinex throughout the scene.[6,44] With all the prior knowledge regarding image contrast, the concept behind this research is that certain functions can be derived to represent the relationship between the physical contrast and the perceived visual contrast while compensating for the variation of the luminance levels in the HDR environment and providing the transformation between HDR and LDR images based on the equivalence of perceived visual contrast. How to generate such numerical functions to serve this purpose is the most critical task for this research.

On the other hand, Burkhardt et al.[50] published an article revealing the relation between physical contrast (Michelson contrast) and perceived visual contrast at the suprathreshold level. The perceived difference between a rectangular bar and its background was defined as the perceived visual contrast. Force-choice psychophysical procedures were used to define the visual contrast equivalence for the background luminance ranging from 0.017 to 200.0 cd/m^2. The results show a nearly symmetrical relation between negative and positive physical contrast to the perception of visual contrast. The most important information in that article is the revealing of the relation between luminance (physical) contrast and corresponding perceived (visual) contrast for rectangular bars viewed under varying background luminance at suprathreshold level. However, only one curve (luminance at 200 cd/m^2) in the original figure was based on fitted data points; the rest of the curves were drawn by eye in the original article in 1984. The estimated data points from the original publication of Burkhardt et al. are listed in Table II. Note that for computational purposes the data range is normalized to between 0 and 1 in this research.

Fechner's law states that the perceived magnitude of a stimulus is proportional to the logarithm of the physical stimulus intensity.[51] The relation between the physical contrast (PC) and the perceived visual contrast (PVC) can be modeled in a general form as

$$PVC = \text{offset} + \text{scalar} * \text{Log}(PC). \qquad (2)$$

With the normalized data between 0.0 and 1.0 for both physical contrast (PC) and perceived visual contrast (PVC), regressions can be applied to the data in Table II, and the results are listed in Table III. Figure 1 shows the fitting results.

Table III. Regression results between physical contrast and relative perceived visual contrast at different levels of background luminance in the form of Eq. (2).

Background luminance (cd/m^2)	Offset	Scalar	R^2
0.017	0.5658	0.4234	0.994
0.17	0.6059	0.4657	0.998
1.55	0.6885	0.5521	0.983
17.00	0.7797	0.6460	0.960
200.00	0.8778	0.7472	0.931

Due to the limitation that a logarithmic function cannot be applied to zero, a special adjustment was made to set the input physical contrast from pure 0 to 0.05 as the regression input. It is also a very practical adjustment to reflect the fact that, when the physical contrast is approaching but not at pure zero (dark), the human perceivable visual contrast will have been at zero already. Important information can be found also for background luminance at 200 cd/m^2, where the estimated perceived visual contrast is predicted to be 0.8778 for the input physical contrast value at 1.0, which implies that higher levels of background luminance can possibly be extended.

Based on the Stevens effect, further modeling was performed in the terms of offset and scalar in Table III as two separate functions of the background luminance values. The results for the two separate regressions of the offset term ($R^2 = 0.984$) and the scalar term ($R^2 = 0.985$) are

$$\begin{aligned}\text{Predicted offset} &= 0.6850 + 0.07879 \\ &\quad * \text{Log(Luminance)} \qquad (3)\\ \text{Predicted scalar} &= 0.5476 + 0.08178 \\ &\quad * \text{Log(Luminance)}. \qquad (4)\end{aligned}$$

Consequently, the perceived visual contrast (PVC) can be combined into one single function with two control parameters, input physical contrast (PC) and background luminance (L_B), as

$$\begin{aligned}PVC &= (0.6850 + 0.07879 * \text{Log}(L_B)) \\ &\quad + (0.5476 + 0.08178 * \text{Log}(L_B)) * \text{Log}(PC), \qquad (5)\end{aligned}$$

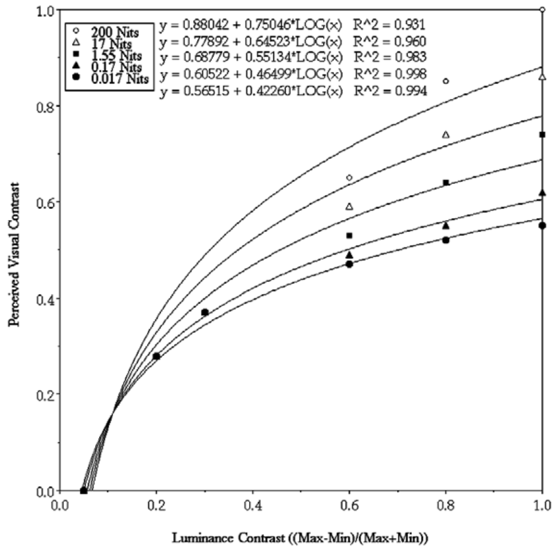

Figure 1. Fitting results from Burkhardt's data points to reveal the estimated relationship between luminance (physical) contrast and perceived visual contrast.

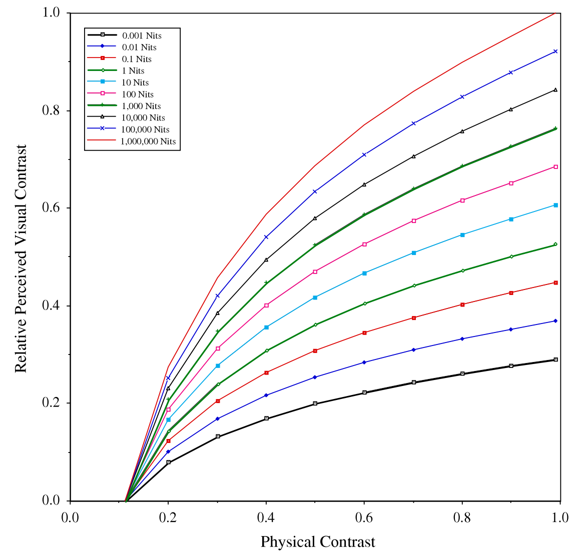

Figure 2. Estimated relative perceived visual contrast curves (versus physical contrast) for luminance levels ranging from 0.001 cd/m^2 (nits) to 1,000,000 cd/m^2.

where *PVC* is the magnitude of the perceived visual contrast, and *PC* is the absolute value of the physical (luminance) contrast defined in Burkhardt[50] as

$$PC = \frac{L_{\max} - L_{\min}}{L_{\max} + L_{\min}}. \tag{6}$$

In the case of incremental bars (the center target is brighter than the background), $L_{\max}$ and $L_{\min}$ are the bar center stimulus (S_C) and background (S_B) luminance, respectively. For every pixel in a complex image the physical contrast becomes

$$PC(x, y) = (S_C(x, y) - S_B(x, y))/(S_C(x, y) + S_B(x, y)). \tag{7}$$

In this article an actual numerical function is derived from Burkhardt's data that can be used to perform the computation from the measurable center/background values to the perceived visual contrast.

It is noted that Burkhardt's[50] original article indicates the output perceived visual contrast at 1.0 when the input contrast is at 1.0 for background luminance at 200 cd/m^2 which is much lower than the range for common HDR images. However, by checking the estimated curve in Fig. 1 the estimated perceived visual contrast for background luminance at 200 cd/m^2 is less than 1.0 when the input physical contrast is 1.0, which implies that the possibility for higher background luminance still follows this relation. To make this estimation close to a real-life situation it is assumed that the maximum luminance could be 1,000,000 cd/m^2 and the minimum luminance 0.001 d/m^2 (9 log units). This makes the maximum physical contrast 0.99999. With the constraint on the extended boundary condition, a new concept of Relative Perceived Visual Contrast (RPVC) extended from Burkhardt's[50] data set is proposed as the following equation.

$$\begin{aligned} RPVC(x, y) &= (0.6850 + 0.07879 * \mathrm{Log}(L_B(x, y))) \\ &\quad + (0.5476 + 0.08178 \\ &\quad * \mathrm{Log}(L_B(x, y))) * \mathrm{Log}((L_{\max}(x, y) \\ &\quad - L_{\min}(x, y))/(L_{\max}(x, y) + L_{\min}(x, y))) - 0.1577, \end{aligned} \tag{8}$$

where $L_B(x, y)$ is the adapting background luminance, and $L_{\max}$ and $L_{\min}$ are the central and background luminance, respectively, whichever is larger or smaller. The RPVC function—estimated relative perceived visual contrast values versus the physical contrast ranging from 0 to 1.0 at luminance levels ranging from 0.001 to 1,000,000 cd/m^2—is plotted in Figure 2. Note that an offset term of −0.1577 is added so that the relative perceived visual contrast value is 1.0 under the extreme condition.

This Eq. (8) provides a computable function between a given physical contrast (*X*-axis) to the relative perceived visual contrast value (*Y*-axis) under a specific adapting background luminance level. Essentially this RPVC mapping function provides contrast mapping functionality associated with the background luminance levels within the assumed range.

HDR IMAGE REPRODUCTION WITH RPVC MAPPING FUNCTION

The objective of image reproduction can be to generate an exact match or a preferred, more pleasing, reproduction.[52] The exact match can be further distinguished as a spectral match, colorimetric match or match of color appearance. For this research on HDR image reproduction the appearance match is intended to preserve our visual experience, for which photography has always been used.

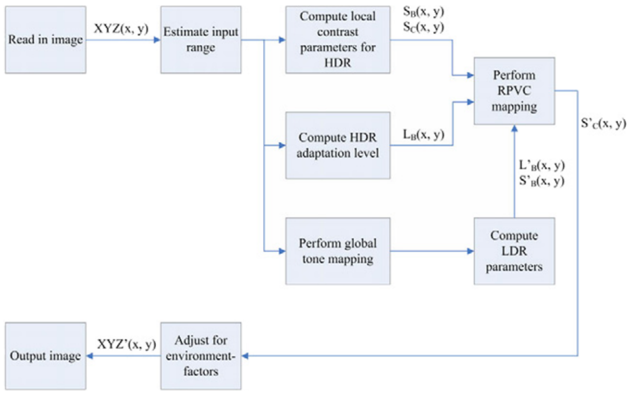

Figure 3. Flowchart of the proposed RPVC HDR processing method.

Hurlbert and Wolf[53] point out that approximately equal appearance can be achieved by equal cone contrasts based on the concept of "constancy of cone contrast". Furthermore, prior psychophysical experiments have demonstrated that for simple configurations the "cone contrast" (the ratios of within-type cone excitation) between a target surface (center) and its immediate area (background) largely determines the color appearance.[54] This matches with findings by Chichilnisky and Wandell[55] that, even though the center–background ratios are different at dissimilar background luminance levels, the appearances can be still equal due to the adjustment role introduced by the background-dependent gain (which can be triggered by the adapting the background luminance level). While the center–background ratios are different at different background luminance levels, the appearances can still be equal due to the adjustment factor introduced by the different gain values in the visual system. Consequently by mapping through the RPVC function, every pixel in the HDR scene can be reproduced in the LDR medium by the equivalence of perceived visual contrast as

$$\begin{aligned} &RPVC_{HDR}(L_B(x,y), S_B(x,y), S_C(x,y)) \\ &= RPVC_{LDR}(L'_B(x,y), S'_B(x,y), S'_C(x,y)), \end{aligned} \tag{9}$$

where five input values

$S_C(x, y)$—central stimulus of the HDR original
$S_B(x, y)$—background stimulus of the HDR original
$L_B(x, y)$—adapting local background luminance of the HDR original
$S'_B(x, y)$—background stimulus of the LDR original
$L'_B(x, y)$—adapting local background luminance of the LDR original

are needed to resolve the unknown LDR central stimulus, $S'_C(x, y)$, which is the reproduced image on the LDR medium.

It is intended to reduce the complexity in processing an HDR image by using this RPVC function. However, many prior publications provided valuable experience revealing important features that must be considered. In this research the global dynamic range compression is performed first in the density (log) domain. A bilateral-type low-pass filter is also incorporated to generate the background stimulus, $S_B(x, y)$, for the HDR scene, since it is needed to preserve the edge details while providing the averaged scene background luminance level. A very special feature found during the model-training stage is the necessity to perform the RPVC mapping in LMS space, not in the regular *XYZ* space, since the LMS coordinate is closer to the photoreceptor operation level. After the local contrast adjustment by the RPVC function, a global compensation for the surround luminance influence in the IPT space is also included to account for both the Bartleson–Breneman[56] and the Hunt[44,57] effects. The complete flow chart is shown in Figure 3. All the processing steps are summarized as follows.

1. *Read in image—Input and convert an HDR file to the absolute colorimetric values of the original scene image, $XYZ(x, y)$.*
2. *Estimate input range—Apply a logarithmic transformation to the input image's absolute XYZ values to establish the reference scene image. Histogram analysis is applied to the reference scene image to locate the maximum and minimum bounds of the dynamic range of the scene. These bounds are taken from 99.8% and 0.2% accumulated percentile to avoid noise. (The white point of the original scene is also estimated here.)*
3. *Compute local contrast parameters for HDR—Transform the original scene image (CIE XYZ values) into the LMS space to generate the central stimulus (Sc) of the scene.*

$$\begin{bmatrix} L \\ M \\ S \end{bmatrix} = \begin{bmatrix} 0.4002 & 0.7076 & -0.0808 \\ -0.2280 & 1.1500 & 0.0612 \\ 0.0000 & 0.0000 & 0.9184 \end{bmatrix} \begin{bmatrix} X \\ Y \\ Z \end{bmatrix}.$$

Process the original scene image signals in the LMS space with the bilateral-type (low-pass) filter to generate the spatially adapted local background stimulus (S_B) of the scene. (This filter is a very important element to avoid the halo effect in the image.)

4. *Compute the HDR adaptation level—Compute the adapting background luminance (L_B) of the original scene by converting the spatially adapted local background stimulus (S_B) of the scene back to an absolute luminance unit. (One major point is that the adapting background luminance is also passed through the bilateral-type filter.)*
5. *Perform global tone mapping—Use a simple linear mapping method to compute a scaling factor (sf) by the ratio of the luminance ranges (Y) between the scene (Y_S) and the reproduced display medium (Y_D) in the intensity domain (log space).*

$$sf = \frac{\log_{10}(Y_{D\max}) - \log_{10}(Y_{D\min})}{\log_{10}(Y_{S\max}) - \log_{10}(Y_{S\min})}.$$

Perform linear mapping in the log space for the image from the scene range to the range of the reproduction *medium. White point mapping is also included by setting the maximum values as the base for scaling and adding back the medium white point as offset:*

$$\mathrm{Log}_{10}(XYZ_d) = (\mathrm{Log}_{10}(XYZ_s) - \mathrm{Log}_{10}(XYZ_{s\,\max})) * sf + \mathrm{Log}_{10}(XYZ_{d\,\max}).$$

(This projection performs the global tone compression to generate the projected medium value. This is output medium dependent.)

6. *Compute the LDR parameters—Transform the projected medium value (in log XYZ space) back to 10 base value to generate the projected adapting background luminance (L'_B) on the reproduction medium. Transform the projected medium value from XYZ back to the LMS space to form the background stimulus (S'_B) of the reproduced medium with the bilateral-type (low-pass) filter.*
7. *Perform RPVC mapping—With the pre-calculated values for: 1. the background stimulus of the scene (S_B), 2. the central stimulus of the scene (Sc), 3. the adapting background luminance of the scene (L_B), 4. the projected adapting background luminance on the reproduction medium (L'_B) and 5. the projected background stimulus on the reproduction medium (S'_B), use the RPVC equation (8) to calculate the central stimulus (S'_C) of the reproduced LDR image in the LMS space for every pixel. (This is the local mapping process similar to that of Meylan[9] in the retina level but in a totally different approach.)*
8. *Adjust for environment factors—Compensate for the surround luminance influence by the averaged luminance of the whole image in the IPT space. The gamma value is set as 1.2, 1.1 and 1.0 for dark, dim and normal lighting conditions, respectively.*
9. *Output image—Convert the images from IPT space to LMS and to XYZ colorimetric space. Convert the reproduced LDR image to the device-dependent signals of the output medium (to the known calibrated display's R, G and B signals, such as sRGB color signals).*

EXPERIMENTAL DESIGN

Two sets of experiments were performed. The first was for an exact visual match with the real scene and to verify this model performance with other HDR models by psychophysical tests. The second was to compare this RPVC model with iCAM06 by processing more HDR sample images in regular photography practice for reference purposes.

In the first set a special configuration was designed to create a high dynamic range scene for performing the visual observation in a dark room. Two cool-white fluorescent light sets at different illumination levels with separated control were used aside (similar to 45/0 viewing geometry) to generate bright and dark sides for the high dynamic range scene. The projection of the light was controlled by four reflectors in front to assure evenness, and the power of the light was also adjustable. A black board was inserted between the two sides and vertical to the observers' view (so an observer is not very aware of its existence) to keep the darker side away from interference by the brighter light on the left side. A Minolta CS-1000 with 50 mm macrolens was used to measure the luminance. The luminance reading on the brightest patch of a Kodak Q-13 gray scale was 317.8 cd/m^2 on the left side. On the right side the luminance reading on the brightest patch of a Kodak Q-13 gray scale was 3.5 cd/m^2. Since the lighting was evenly distributed on the gray chart, the luminance on the darkest patch on the right side can be estimated as 0.045 cd/m^2 by its reflectance ratio. Part of the lighting configuration (the left side is the brighter side) is shown in Figure 4.

Figure 4. The lighting configuration used in the first experiment. The cool-white fluorescent light set on the left provides much higher illumination than the one on the far right (not seen) to generate HDR conditions.

A Canon 5D digital camera with a Canon EF 50 mm/2.8 macrolens was used to capture the image. Three pictures of 1/12, 1/3 and 1.3 second exposures at f8.0 were taken at ISO 100. Adobe Photoshop CS3 was used to generate the .hdr file to be processed by a MATLAB program. These original images are shown in Figure 5. An Eizo ColorEdge CG21 21-inch LCD monitor calibrated by a Gretag i1 pro spectral-colorimeter to D65 white point and Gamma 2.2 was used to display the test images. Its displayable area was 1600 × 1200 pixels at 0.27 mm/pixel pitch and the white point and the black point were measured as 144.2 cd/m^2 and 0.34 cd/m^2, respectively. (These values were used as the parameters for the output LDR medium in the first set of the experiments.) The observers sat in the position where the viewing angles to the images shown on the LCD and to the real scene were the same, as shown in Figure 6. The observers were situated in a dark room and could view the LCD display and the scene back and forth successively in two perpendicular viewing directions.

Six other HDR image-reproduction models and this RPVC model as listed in Table IV were used to generate the test images. The executable programs from the attached CD in Reinhard et al.'s publication[17] in their default settings were used for the first five models. The iCAM06 MATLAB program from RIT's web site was used to process the .hdr file on a Microsoft Window XP platform. All seven reproduced images are shown in Figure 7.

In total, 37 observers participated in the visual assessment by the paired comparison method.[58,59] The observers

(1) Over-exposure (1.3s f8.0)

(2) Normal exposure (1/3s, f8.0)

(3) Under-exposure (1/12s, f8.0)

Figure 5. The original images: (1) over-exposure, (2) normal exposure, (3) under-exposure.

Figure 6. The viewing environment for the paired comparison between the real HDR scene and the reproduced LDR images. (The room light was turned on here for illustration.) The observer can turn 90° to view each side back and forth.

Table IV. List of the HDR models used in the first experiment.

Model no.	HDR model	Reference
1	Local contrast	Ashikhmin[25]
2	Bilateral filtering	Durand–Dorsey[26]
3	Photographic operator	Reinhard[24]
4	Photoreceptor	Reinhard–Devlin[28]
5	Retinex (Rahman)	Rahman[8]
6	iCAM06	Fairchild,[12,13] Kuang[14]
7	RPVC	This article

(1) Local contrast

(2) Bilateral filtering

(3) Photographic operator

(4) Photoreceptor

(5)Rahman Retinex

(6) iCAM06

(7) RPVC

Figure 7. The seven HDR images reproduced in the first experiment.

were instructed to pick one of the two images on the LCD monitor, considered to visually resemble the real scene most, in the same room during three separate rounds. The criteria

Table V. List of resulting Z-scores for all three rounds of real-scene tests.

No.	HDR model	Z-scores Overall	Bright area	Dark area
1	Local contrast	0.63	0.76	0.3
2	Bilateral filtering	−1.37	−1.31	−0.7
3	Photographic operator	−1.97	−1.85	−1.31
4	Photoreceptor	−0.59	−0.75	−0.06
5	Retinex (Rahman)	−0.07	0.03	−0.47
6	iCAM06	1.85	1.86	1.01
7	RPVC	1.52	1.25	1.23

given for all three rounds were (a) overall reproduction, (b) reproduction in the bright region and (c) reproduction in the dark region. There was no time limit for the observers in performing the tests.

The second set of experiments was performed purely for reference since the design principle of this RPVC model is to reproduce the LDR image perceptually accurate to the scene; therefore it is not practical to carry out any comparison with other HDR models without the actual scene being presented at the same time. Nevertheless, the results processed by iCAM06 are included together to provide a general reference. Images taken by the author recently and publicly available test images from RIT Mark Fairchild's HDR Photographic Survey[60] were used to generate the LDR images. For the target LDR medium in the RPVC process the luminance range was set to 150 and 1 cd/m^2 for the white and the black points, similar to standard RGB encoding (sRGB)[61], to make it closer to common color printing conditions or normal computer displays nowadays. All these images were processed through a MATLAB program under Version 7.10.0 on an Intel Core2 Quad Q9550 PC at 2.83 GHz with 3.25 GB RAM under Microsoft Windows XP Service Pack 3. The optimized C code was executed with parallel computing feature in an NVIDIA Tesla C1060 GPU card. The respective computation time was also recorded for comparison.

RESULTS AND ANALYSIS

The results of the paired comparison in the first set of experiments for all three rounds were analyzed using Thurstone's Law, Case V,[59] as summarized in Table V. The resulting Z-scores with error bar within the 95% confidence limits[62] are shown in Figures 8–10, for overall, bright area and dark area, respectively.

The results of the overall performance shown in Fig. 8 indicate that the iCAM06 (model No. 6) is ranked first; however, it is not significantly better than the RPVC (model No. 7) within the 95% confidence interval. The local contrast (model No. 1) comes third, and then Rahman Retinex, photoreceptor, photographic operator and bilateral filtering, significantly different.

The results of the test in the bright region as shown in Fig. 9 indicate that iCAM06 has significantly the best performance within the 95% confidence interval, with the RPVC model coming second. The local contrast (model No. 1) comes third, and then, in order, Rahman Retinex, photoreceptor, photographic operator and bilateral filtering. They all appear significantly different within the 95% confidence interval.

The nature of the HDR environment causes the image in the darker region to contain very important visual information. When evaluating the dark region, the RPVC model is ranked first, but it is not significantly better than iCAM06 within the 95% confidence interval. Moreover, the RPVC model and iCAM06 are in the same group, which is significantly better than the other models, similarly to

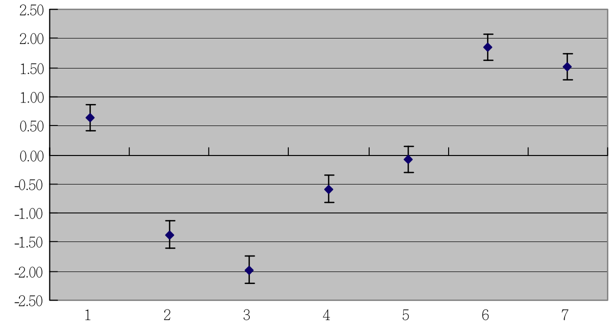

Figure 8. Results of the comparison for the overall reproduction in Z-scores: 1. local contrast, 2. bilateral filtering, 3. photographic operator, 4. photoreceptor, 5. Rahman Retinex, 6. iCAM06, 7. RPVC.

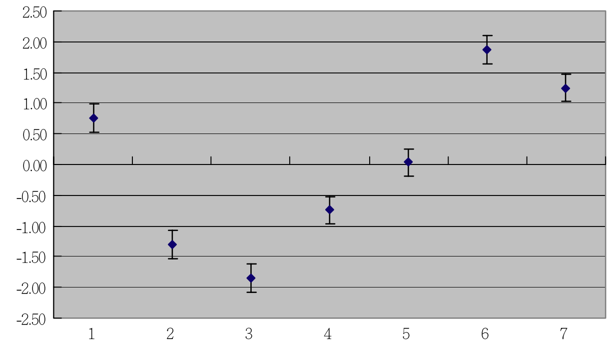

Figure 9. Results of the comparison for the bright region in Z-scores: 1. local contrast, 2. bilateral filtering, 3. photographic operator, 4. photoreceptor, 5. Rahman Retinex, 6. iCAM06, 7. RPVC.

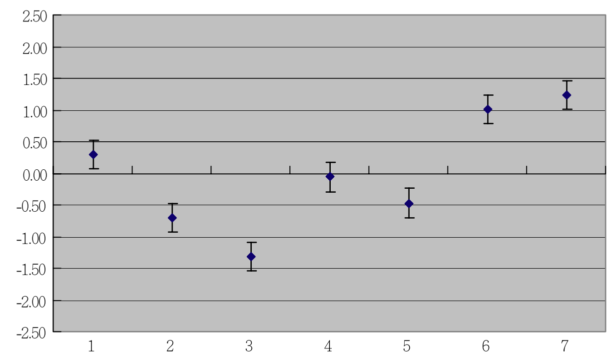

Figure 10. Results of the comparison for the dark region in Z-scores: 1. local contrast, 2. bilateral filtering, 3. photographic operator, 4. photoreceptor, 5. Rahman Retinex, 6. iCAM06, 7. RPVC.

(a) iCAM06 (gamma 1.1) (b) RPVC

Figure 11. A foggy-night HDR scene processed by (a) iCAM06 and (b) the RPVC model. It is important to see that there is no halo problem on the brightest spot. (Radiance data courtesy Jack Tumblin, Northwestern University.)

(a) iCAM06 (gamma 1.2)

(b) RPVC

Figure 12. A typical night street HDR scene (Frontier) processed by (a) iCAM06 and (b) the RPVC model. It is important to note the similar hue on the neon signs for both outputs. (Original image from Mark Fairchild's HDR Photographic Survey.[60]) .

the results of overall test. The local contrast model comes third, but it is not significantly better than the fourth, the photoreceptor model. The Rahman Retinex comes fifth, but it is not significantly better than bilateral filtering, in sixth place. Finally, the photographic operator is in a separate

(a) iCAM06 (gamma 1.1) (b) RPVC

Figure 13. A typical dawn HDR scene processed by (a) iCAM06 and (b) the RPVC model. The main point is that the distribution of the tone has to be realistic.

(a) iCAM06 (gamma 1.0)

(b) RPVC

Figure 14. An early morning HDR scene processed by (a) iCAM06 and (b) the RPVC model. It is before sunrise; therefore the contrast is low.

group. The fine difference in the dark region seems to be not that obvious to the observer as there is more overlapping in the 95% confidence interval for the dark region test than in the other two tests.

The photoreceptor model (model No. 4) shows a greater improvement in its performance when the dark area is evaluated. This may imply that considering the characteristics of the photoreceptor in a dim situation can

(a) iCAM06 (gamma 1.1)

(b) RPVC

Figure 15. A typical sunrise HDR scene processed by (a) iCAM06 and (b) the RPVC model. If the contrast were too high, it would appear too sharp as well.

(a) iCAM06 (gamma 1.0)

(b) RPVC

Figure 17. A typical outdoor HDR scene (Peck Lake)[60] processed by (a) iCAM06 and (b) the RPVC model. It is important to see a smooth gradation on the white clouds. (Original image from Mark Fairchild's HDR Photographic Survey[60]).

(a) iCAM06 (gamma 1.0) (b) RPVC

Figure 16. A daylight HDR scene processed by (a) iCAM06 and (b) the RPVC model. The white balance shall be kept on the white wall.

improve the reproduction to become closer to the real scene. It may also explain why the RPVC model performs well in the darker region since the cone contrast functionality is considered, and different levels of luminance are modeled more precisely on the RPVC function.

In the meantime, the local contrast model (model No. 1) consistently takes third place in all three rounds, which reconfirms the trend that the contrast attribute plays an important role in HDR image reproduction. It may be the consideration of the processing signals in the LMS color space or the compensation in the IPT color space for the Hunt effect in the RPVC model that makes the difference from the earlier HDR models, like the local contrast operator (model No. 1) and the photoreceptor model (model No. 4).

The nonlinear tone compression functions of iCAM06 are similar to those in CIECAM02, with a slightly modified user-controllable power value in the range from 0.6 to 0.85.[15] However, learning from a concept like the transducer function,[63] the RPVC model would change the mapping merit according to the adapting luminance levels, which adjusts the local contrast gain effectively. This can be a simple but powerful feature in this RPVC model. Calabria and Fairchild[45] confirmed the influence of image lightness, chroma and sharpness transformations on perceived image contrast. In this RPVC model it might be the other way around, namely that the contrast adjustment feature enhances the lightness, chroma and sharpness characteristics of the image. It may be for this reason also that the RPVC model performs better in the dark region. Meanwhile, iCAM06 has more elaborate handling in chromatic adaptation and the surround influence, which might be a contributing reason why iCAM06 performs better than the RPVC model in the bright region. Furthermore, since the original Burkhardt data only had a background luminance level of up to 200 cd/m^2,

(a) iCAM06 (gamma 1.0)

(b) RPVC

Figure 18. A panoramic view taken at noon. HDR scene processed by (a) iCAM06 and (b) the RPVC model. The lighting in this scene is very extreme. (Original photos courtesy Wen-Pin Chang, Splendid Studio Co., Ltd.)

(a) iCAM06 (gamma 1.0)

(b) RPVC

Figure 19. A typical afternoon indoor HDR scene processed by (a) iCAM06 and (b) the RPVC model. The main difference is that the sky should be kept white.

(a) iCAM06 (gamma 1.0)

(b) RPVC

Figure 20. Sunshine after rain. HDR scene processed by (a) iCAM06 and (b) the RPVC model. This is a very difficult lighting situation for regular photography. However, both models perform very well.

the extension of the luminance level into much higher levels might not be so precise.

The resulting LDR images from the second part of the experiment are listed in Figures 11–22. They are deliberately selected for various lighting conditions and at different times of day to simulate the color temperature and luminance level changes in nature. Both iCAM06 and the RPVC model were used to process these HDR images. In general the reproduced images from the RPVC model are similar to the results from iCAM06. The process times needed by iCAM06 and the RPVC model are listed in columns 3 and 4 of Table VI. The local contrast-based feature in the RPVC model required more computation effort with the regular bilateral filter, as shown in column 4 of Table VI. However, if the regular bilateral filter is replaced by iCAM06's optimized bilateral filter (piecewise linear approximation and nearest-neighbor downsampling),[15] the process time can be significantly reduced, as shown in column 5 of Table VI. When the RPVC

Table VI. List of process times (in seconds) by iCAM06 and by the RPVC model, as well as by the RPVC model with iCAM06's optimized bilateral filter, and by the RPVC model in optimized C code with parallel processing in experiment 2.

Test image	Image size (Pixels)	By iCAM06's MATLAB code	By the RPVC with a regular bilateral filter in MATLAB	By the RPVC with iCAM06's optimized bilateral filter in MATLAB	By the RPVC in optimized Visual C code with parallel processing
Fig. 11	376 × 556	4.1	27.0	4.7	1.5
Fig. 12	1510 × 1003	30.6	185.4	39.2	10.3
Fig. 13	531 × 799	7.0	52.7	8.8	2.9
Fig. 14	1510 × 1005	23.4	186.6	30.5	10.0
Fig. 15	1511 × 1007	21.4	186.0	26.8	10.2
Fig. 16	530 × 797	7.1	53.5	9.2	2.9
Fig. 17	697 × 443	14.3	45.4	15.5	2.1
Fig. 18	1510 × 306	7.3	62.4	8.9	3.2
Fig. 19	1510 × 1005	24.5	183.8	30.7	10.1
Fig. 20	1510 × 1006	24.2	185.8	31.8	10.2
Fig. 21	1510 × 1007	21.4	185.2	29.0	10.0
Fig. 22	512 × 768	6.3	49.3	7.7	2.7

(a) iCAM06 (gamma 1.1)

(b) RPVC

Figure 21. A sunset HDR scene processed by (a) iCAM06 and (b) the RPVC model. The gradation of the sky is well kept.

model is implemented using C code with parallel processing optimization, the processing time can be further reduced, as shown in column 6 of Table VI. The resulting images (Figs. 11b–22b) are processed by the RPVC model with a regular bilateral filter.

(a) iCAM06 (gamma 1.1)   (b) RPVC

Figure 22. An indoor scene processed by (a) iCAM06 and (b) the RPVC model. This image (memorial_hires)[17] is the most essential test image to show the general characteristics.

CONCLUSIONS

The major challenge for HDR image reproduction is to maintain the visual experience of the HDR scene while reproducing the image in an LDR medium by a certain tone-mapping algorithm. This research takes a new approach that keeps the visual contrast consistent between the HDR scene and the LDR reproduction by mapping through the proposed relative perceived visual contrast (RPVC) function. This RPVC function is derived in this study from an article published by Burkhardt et al. in 1984, in which the local physical contrast and adapting background luminance are the primary input-control parameters to compute the relative perceived visual contrast value. It is based on the theory that the perceived visual contrast would increase while the adapting background luminance increased, which is also known as the Stevens effect.

Several essential features, such as an edge-preserving bilateral low-pass filter and density domain linear mapping, as well as computation in LMS and IPT spaces, are also incorporated into this RPVC model. By processing through this model, equivalent visual contrast can be achieved for every image pixel between the HDR scene and the LDR medium even though their local physical contrast values are different. It is intended to make this new RPVC model less complicated and easier to use by not having to select any extra user-control parameters.

A special lighting-controlled configuration in a dark room was built to create a real HDR scene with various objects for model training and cross-model evaluation. The psychophysical comparison between this RPVC model and the other previously published HDR models in their respective default settings (local contrast, bilateral filtering, photographic operator, photoreceptor, Rahma Retinex, iCAM06) reveals a moderate performance of this RPVC model—for reproduction in the bright region iCAM06 had the best performance while the RPVC model came second; in overall reproduction, iCAM06 was ranked the highest, but it was not significantly better than the RPVC model; for reproduction in the dark region, the RPVC model was ranked the highest, but it was not significantly better than iCAM06; the local contrast model always came third in all three regions.

The reproduced LDR images in the second part of the experiment provide a good sense of reference for applying this RPVC model in comparison to iCAM06 under various lighting conditions in real-world photography practice. Even though there is no real scene provided to be compared with, the common features for good photographic practice, such as gray balance, tone rendition and sharpness, can be good indications for the readers to judge.

This research is based on the assumption that local contrast adjustment is an important factor in keeping consistent visual experience between HDR and LDR imaging. Even though the local contrast feature in the RPVC model would need extra processing time, it may not be an issue with the availability of parallel processing in newer computer hardware. In general, the results of the experiments confirm that this approach is feasible and that the RPVC model is nearly as effective as iCAM06 in handling HDR images.

ACKNOWLEDGMENT

The authors express their particular thanks to the reviewers for valuable comments, Mr. H. Erdmann-Harenberg for making this research more comprehensible, and Ms. Eva Lin for great assistance. This research is partially supported by the Taiwan National Science Council and a grant from the TELDAP agency (project number 100-2631-H-034-001).

REFERENCES

[1] A. Adams, *The Negative* — The Second Volume of the Ansel Adams Photography Series, Tenth paperback printing (Little, Brown and Company, 2002).

[2] A. Adams, *The Print* — The Third Volume of the Ansel Adams Photography Series, Tenth paperback printing (Little, Brown and Company, 2003).

[3] A. Adams, *The Camera* — The First Volume of the Ansel Adams Photography Series, Eleventh paperback printing (Little, Brown and Company, 2004).

[4] A. Adams, *Examples: The Making of 40 Photographs*, 1st ed. (Little, Brown and Company, 1983) p. 105.

[5] G. S. Miller and C. R. Hoffman, Illumination and Reflection Maps: Simulated Objects in Simulated and Real Environments, SIGGRAPH 84 Course Notes for Advanced Computer Graphics Animation (July, 1984).

[6] E. H. Land and J. J. McCann, "Lightness and retinex theory," J. Opt. Soc. Am. **61**, 1–11 (1967). Reprinted in *Edwin H. Land's Essays*, Volume III, Color Vision (IS&T, Springfield, VA 1993), pp. 73–84.

[7] H. Kotera and M. Fujita, "Appearance improvement of color image by adaptive scale-gain retinex model," *Proc. IS&T/SID 10th Color Imaging Conf.* (IS&T, Springfield, VA 2002), pp. 166–171.

[8] Z. Rahman, D. J. Jobson, and G. A. Woodell, "Retinex processing for automatic image enhancement," J. Electron. Imaging **13**, 100–110 (2004).

[9] L. Meylan, D. Alleysson, and S. Susstrunk, "Model of retina local adaptation for the tone mapping of color filter array images," J. Opt. Soc. Am. **24**, 2807–2816 (2007).

[10] L. Wang, T. Horiuchi, and H. Kotera, "High dynamic range image compression by fast integrated surround retinex model," J. Imaging Sci. Technol. **51**, 34–43 (2007).

[11] X. Zhang and B. A. Wandell, "A spatial extension to CIELAB for digital color image reproduction," Proc. SID Symp. **27**, 731–734 (1996).

[12] M. D. Fairchild and G. M. Johnson, "Meet iCAM: a next-generation color appearance model," *Proc. IS&T/SID 10th Color Imaging Conf.* (IS&T, Springfield, VA 2002), pp. 33–38.

[13] M. D. Fairchild and G. M. Johnson, "iCAM framework for image appearance, differences and quality," J. Electron. Imaging **13**, 126–138 (2004).

[14] J. Kuang and M. D. Fairchild, "iCAM06, HDR and Image Appearance," *Proc. IS&T/SID 15th Color Imaging Conf.* (IS&T, Springfield, VA 2007), pp. 249–254.

[15] J. Kuang, G. M. Johnson, and M. D. Fairchild, "iCAM06: a refined image appearance model for HDR image rendering," J. Vis. Commun. Image Rep. **18**, 406–414 (2007).

[16] J. Tumblin and H. Rushmeier, "Tone reproduction for computer generated images," IEEE Comput. Graph. Appl. **13**, 42–48 (1993).

[17] E. Reinhard, G. Ward, S. Pattanaik, and P. Debevec, *High Dynamic Range Imaging*, 1st ed. (Morgan Kaufmann Publishers, Elsevier Inc., 2006).

[18] E. Reinhard, W. Heidrich, P. Debevec, S. Pattanaik, G. Ward, and K. Myszkowski, *High Dynamic Range Imaging*, 2nd ed. (Morgan Kaufmann, 2011).

[19] K. Chiu, M. Herf, P. Shirley, S. Swamy, C. Wang, and K. Zimmerman, "Spatially non-uniform scaling functions for high contrast images," Proc. Graph. Interface 245–244 (1993).

[20] G. Ward, "A contrast-based scale factor for luminance display," *Graphics Gems*, edited by P. Heckbert, 4th ed. (Academic Press, Boston, 1994), pp. 415–421.

[21] J. A. Ferwerda, S. N. Pattanaik, P. Shirley, and D. P. Greenberg, "A model of visual adaptation for realistic image synthesis," ACM Proc. SIGGRAPH 249–258 (1996).

[22] G. Ward-Larson, H. Rushmeier, and C. Piatko, "A visibility matching tone reproduction operator for high dynamic range scenes," IEEE Trans. Vis. Comput. Graph. **3**, 291–306 (1997).

[23] S. N. Pattanaik, J. A. Ferwerda, M. D. Fairchild, and D. P. Greenberg, "A multiscale model of adaptation and spatial vision for realistic image display," ACM Proc. SIGGRAPH 287–298 (1998).

[24] E. Reinhard, M. Stark, P. Shirley, and J. Ferwerda, "Photographic tone reproduction for digital images," ACM Proc. SIGGRAPH 249–256 (2002).

[25] M. Ashikhmin, "A tone mapping algorithm for high contrast images," *Proc. 13th Eurographics Workshop on Rendering* (Pisa, Italy, 2002), pp. 145–155.

[26] F. Durand and J. Dorsey, "Fast bilateral filtering for the display of high-dynamic-range images," ACM Proc. SIGGRAPH 257–266 (2002).

[27] R. Fattal, D. Lischinski, and M. Werman, "Gradient domain high dynamic range compression," ACM Trans. Graph. **21**, 249–256 (2002).

[28] E. Reinhard and K. Devlin, "Dynamic range reduction inspired by photoreceptor physiology," IEEE Trans. Vis. Comput. Graph. **11**, 13–24 (2005).

[29] Z. Lu and S. Rahardja, "Realistic HDR tone-mapping based on contrast perception matching," *Proc. 16th IEEE, Int'l. Conf. on Imaging Processing (ICIP), 2009*, pp. 1789–1792.

[30] M. J. Shyu and Y. Miyake, "High dynamic image reproduction using a visual contrast mapping model," *Proc. IS&T/SID 17th Color Imaging Conf.* (IS&T, Springfield, VA, 2009), pp. 290–295.

[31] N. Moroney and I. Tastl, "Comparison of retinex and iCAM for scene rendering," J. Electron. Imaging **13**, 139–145 (2004).
[32] P. Ledda, A. Chalmers, T. Troscianko, and H. Seetzen, "Evaluation of tone mapping operators using a high dynamic range display," ACM Trans. Graph. **24**, 640–648 (2005).
[33] J. Kuang, C. Liu, G. M. Johnson, and M. D. Fairchild, "Evaluation of HDR image rendering algorithms using real-world scenes," *Proc. ICIS '06, Int'l. Congress of Imaging Science* (2006), pp. 265–268.
[34] M. Cadik, M. Wimmer, L. Neumann, and A. Artusi, *Proc. Pacific Graphics* (National Taiwan University Press, Taiwan, 2006), pp. 35–44.
[35] A. Yoshida, V. Blanz, K. Myszkowski, and H.-P. Seidel, "Testing tone mapping operators with human-perceived reality," J. Electron. Imaging **16**, 1–14 (2007).
[36] J. Kuang, H. Yamaguchi, C. Liu, G. M. Johnson, and M. D. Fairchild, "Evaluating HDR rendering algorithms," ACM Trans. Appl. Perception **4**, (2007) Article 1.
[37] B. Annighofer, T. Tajbakhsh, and R. Grigat, "Prediction of results from subjective evaluation of real-time-capable tone-mapping operators applied to limited high-dynamic-range images," J. Electron. Imaging **19**, 011015 (2010).
[38] R. W. G. Hunt, Why is Black and White So Important in Colour? *Colour Imaging, Vision and Technology*, edited by L. W. MacDonald and M. R. Luo, (John Wiley and Sons, 1999), p. 13.
[39] A. A. Michelson, *Studies in Optics* (University of Chicago Press, Chicago, 1927).
[40] E. Peli, "Contrast in complex images," J. Opt. Soc. Am. A **7**, 2032–2040 (1990).
[41] M. D. Fairchild, "Considering the surround in device-independent color imaging," Color Res. Appl. **20**, 352–363 (1995).
[42] C. Liu and M. D. Fairchild, "Measuring the relationship between perceived image contrast and surround illumination," *Proc. IS&T/SID 12th Color Imaging Conf.* (IS&T, Springfield, VA 2004, 2004), pp. 282–288.
[43] A. Rizzi, T. Algeri, G. Medeghini, and D. Marini, "A proposal for contrast measure in digital image," *Proc. CGIV 2004: The Second European Conf. on Colour Graphics, Imaging and Vision* (IS&T, Springfield, VA 2004), pp. 187–192.
[44] M. D. Fairchild, *Color Appearance Model*, 2nd ed. (John Wiley and Sons, 2005).
[45] A. J. Calabria and M. D. Fairchild, "Perceived image contrast and observer preference I. The effects of lightness, chroma, and sharpness manipulations on contrast perception," J. Imaging Sci. Technol. **47**, 479–493 (2003).
[46] A. J. Calabria and M. D. Fairchild, "Perceived image contrast and observer preference II. Empirical modeling of perceived image contrast and observer preference data," J. Imaging Sci. Technol. **47**, 495–508 (2003).
[47] J. C. Stevens and S. S. Stevens, "Brightness functions: effect of adaptation," J. Opt. Soc. Am. **53**, 375–385 (1963).
[48] N. Ohta and A. R. Robertson, *Colorimetry: Fundamentals and Applications* (John Wiley and Sons, 2005).
[49] B. A. Wandell, *Foundation of Vision* (Sinauer Associates, 1995).
[50] D. A. Burkhardt, J. Gottesman, D. Kersten, and G. E. Legge, "Symmetry and constancy in the perception of negative and positive luminance contrast," J. Opt. Soc. Am. **1**, 309–316 (1984).
[51] E. Peli, "Search of a contrast metric: matching the perceived contrast of Gabor patches at different phases and bandwidths," Vision Res. **37**, 3217–3224 (1997).
[52] R. S. Berns, *Billmeyer and Saltzman's Principles of Color Technology*, 3rd ed. (John Wiley and Sons, 2000).
[53] A. Hurlbert and K. Wolf, "The contribution of local and global cone-contrasts to colour appearance: a retinex-like model," *Proc. SPIE 4662* (2002), pp. 286–297.
[54] M. P. Lucassen and J. Walraven, "Quantifying color constancy –evidence for nonlinear processing of cone-specific contrast," Vision Res. **33**, 739–757 (1993).
[55] E. Chichilnisky and B. A. Wandell, "Photoreceptor sensitivity changes explain color appearance shifts induced by large uniform backgrounds in dichoptic matching," Vision Res. **35**, 239–254 (1995).
[56] C. J. Bartleson and E. J. Breneman, "Brightness perception in complex field," J. Opt. Soc. Am. **57**, 953–957 (1967).
[57] R. W. G. Hunt, "Light and dark adaptation and the perception of color," J. Opt. Soc. Am. **42**, 190–199 (1952).
[58] C. J. Bartleson and F. Grum, Eds., *Optical Radiation Measurements*. vol. 5, Visual Measurements (Academic Press, New York, 1984).
[59] P. G. Engeldrum, *Psychometric Scaling* (Imcotek Press, Winchester, MA, 2000).
[60] M. D. Fairchild, on RIT's website for HDR Photographic Survey www.cis.rit.edu/fairchild/HDR.html, accessed March 2012.
[61] M. Stokes, M. Anderson, S. Chandrasekar, and R. Motta, A Standard Default Color Space for the Internet — sRGB, www.w3.org/Graphics/Color/sRGB.html, accessed September 2008.
[62] E. Montag, "Louis Leon Thurstone in Monte Carlo: creating error bars for the method of paired comparison," *Proc. SPIE 5294* (2004), pp. 222–230.
[63] P. G. Barten, *Contrast Sensitivity of the Human Eye and its Effects on Image Quality* (SPIE Press, Washington, 1999).